

Frequency Scanning Fibre Interferometer for Absolute Distance Measurements over a Large Target Area

Yanmei Han, Armin Reichold, Colin Perry, Richard Bingham
John Adam Institute and Physics Department, University of Oxford

The Linear Collider Alignment and Survey (LiCAS) project aims to establish the reference survey network of the ILC (International Linear Collider) by measuring the relative positions of survey reference markers, located in a regular sequence along the tunnel walls of the ILC. A fibre distance sensor has been developed by the Oxford LiCAS group to measure the coordinates of the tunnel markers. It exploits the frequency scanning interferometry (FSI) technique, supplying a reference interferometer and multiple measurement interferometers from one shared frequency scanning laser source. In the measurement interferometer a fibre tip without any optic is used to launch and receive light to perform absolute distance measurements over a large target area. In this paper, calculations based on the Gaussian field distribution are presented, which predict the efficiency of the reflected light from the tunnel marker coupled back to the launching fibre. The high gain and low noise photo-detection unit is described. Preliminary measurement results are reported.

1. INTRODUCTION

In order to collide highly focused beams with dimensions of the order of nanometres, the International Linear Collider (ILC) demands very precise alignment of its components [1][2]. The required accuracy is $200\mu\text{m}$ ($500\mu\text{m}$) vertical (horizontal) over a 600m distance, which cannot be obtained by conventional surveying techniques [2]. This led to the development of the Rapid Tunnel Reference Surveyor (RTRS) by the Oxford LiCAS group in collaboration with the DESY applied geodesy group. The RTRS aims to establish the reference survey network of the ILC, it consists of 6 measurement cars which perform measurements between neighbouring cars and the tunnel reference markers, located in a regular sequence along the tunnel walls of the ILC[3][4].

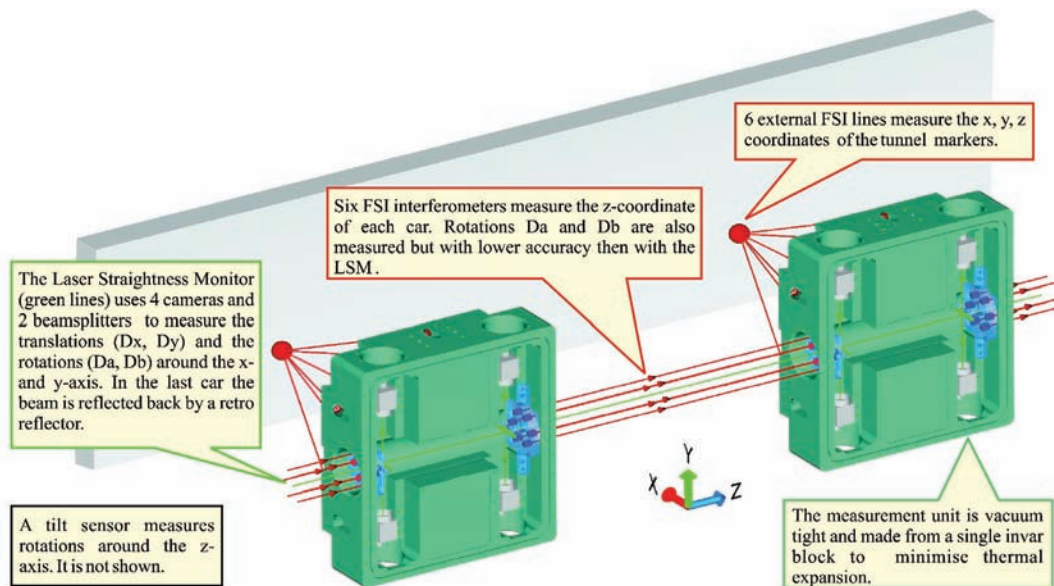


Figure 1: Sensor configuration between two measurement units of the RTRS

Figure 1 depicts the sensor configuration between two measurement cars of the RTRS, more details of the RTRS measurement principle can be found in [4] [5]. Among all these measurements, distances between the two measuring units along the tunnel wall and the co-ordinates of the tunnel markers in respect of the measuring car are measured by frequency scanning interferometry (FSI) technique.

1.1. Principle of the FSI measurement

FSI is an absolute distance measurement technique developed at Oxford for the ATLAS particle detector, measuring the phase change of an interferometer as the laser frequency is scanned [6]. There must be a stable reference interferometer (RI) with a known optical path difference (OPD) L , sharing the same frequency scanning laser source with the measurement interferometer (MI) with an unknown OPD D .

When the frequency of the laser sweeps over an interval $\Delta\nu$, the induced phase changes in the RI and MI are

$$\Delta\Phi = \frac{2\pi}{c} L\Delta\nu \quad (1)$$

and

$$\Delta\Theta = \frac{2\pi}{c} D\Delta\nu \quad (2)$$

respectively.

Provided that both interferometer OPDs do not change during the frequency scan, the ratio of phase changes of the interferometers, q , can be expressed by

$$q = \frac{\Delta\Phi}{\Delta\Theta} = \frac{L}{D}. \quad (3)$$

Then the unknown measurement interferometer OPD can be calculated using

$$D = \frac{L}{q}. \quad (4)$$

Thus the basic aim in an FSI measurement is to find q for each interferometer in order to determine D . For a more detailed description of the algorithm used to extract D see [7].

1.2. FSI measurement system in LiCAS

The FSI system proposed for LiCAS is shown schematically in figure 2. The key device of the FSI is a tunable laser. Here a telecom tunable laser (Agilent 81640A) is exploited, which can tune continuously at speeds of up to 40nm/s over any 30nm section in a wavelength range from 1510nm to 1640nm. The maximum output power of the Agilent 81640A laser is 1.95mW. In order to carry out multiple line measurements, an Erbium Doped Fibre Amplifier (EDFA) (KPS-BT-C-21-Bo) is used to amplify the light from the laser. It can amplify the laser up to 100mW at an optical bandwidth of 1535 – 1565nm, providing a scalable and cost effective solution. The tunable laser and EDFA are controlled via GPIB, thus the wavelength bandwidth, sweeping speed and output light power can be set remotely.

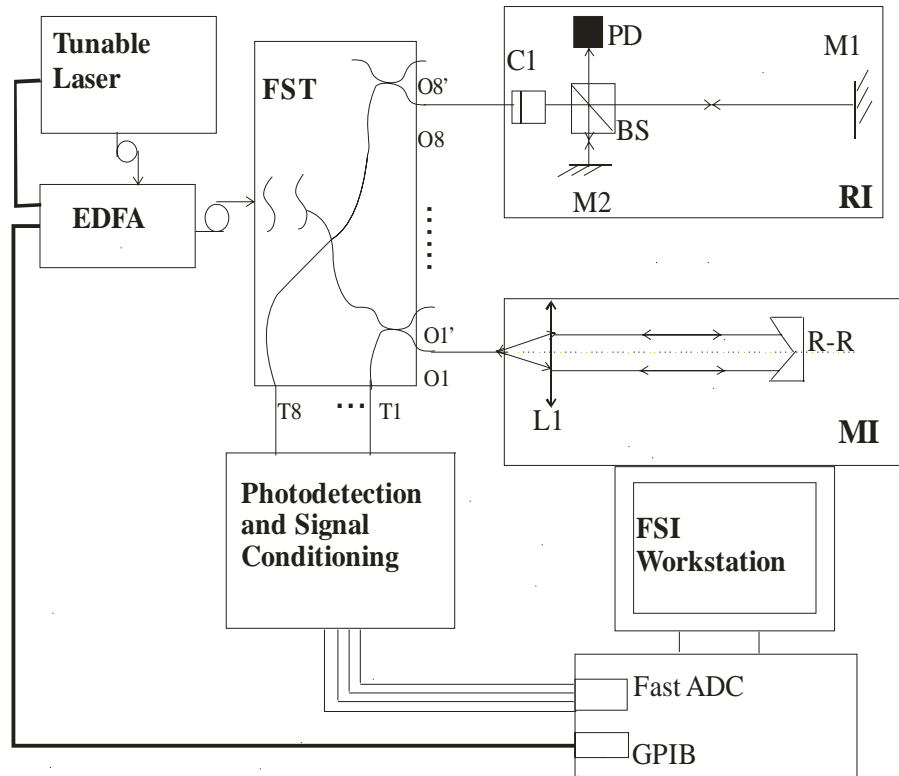


Figure 2: The schematic diagram of the laboratory FSI system for LiCAS. FST: fibre splitter tree; O1, O1'...O8, O8': 16 output channels of the FST; T1...T8: 8 feedback channels of the FST; RI, reference interferometer; C1: collimation optics; BS: beam splitter; PD: Photodiode; M1, M2, reflecting mirrors; MI: measurement interferometer; L1: collimation lens; R1: retro-reflector.

The output light of the EDFA is sent to a fibre splitter tree (FST) which splits the light into many output channels, allowing simultaneous length measurements to be made by comparison with the same reference interferometer RI. Single mode fibre Corning SMF-28 is used here for light delivery. Interference signals from the RI and MIs are fed to a FSI workstation for analysis.

1.3. Requirements for the external short line measurement

As shown in figure 1, the measurement of the x, y, z co-ordinates of the tunnel markers in respect of the measuring car is performed by a set of 6 FSI distance measurements in the form of a cone. The combination of the 6 lines can over-determine the 3D co-ordinates. The tunnel markers are sphere mounted retro-reflectors of 1 inch clear aperture. The distance between the car and the retro-reflector is 400mm~500mm, and the retro-reflector roams in a $50 \times 50 \times 50 \text{mm}^3$ cube, as shown in figure 3. At a measurement distance of 420mm, the retro-reflector can be about 33mm off-axis. Then the crucial requirement for the external FSI is to cover a large area of about 70mm diameter.

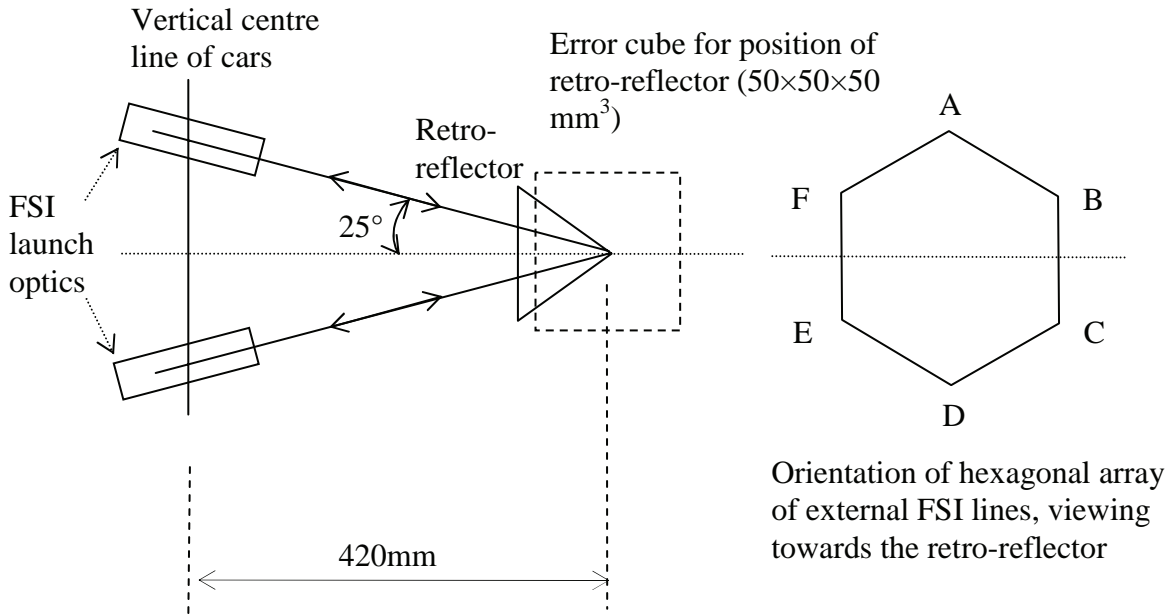


Figure 3: Optical arrangement of the external short FSI lines (six per car)

Possible solutions for the external FSI are listed in table 1.

Table 1: Possible solutions for the external FSI lines

Solution	Method	Characteristic
1	Use a collimated beam of ~70mm diameter	Large optics
2	Steer a collimated beam of a small diameter	High return power, automatic moving parts
3	Use the beam directly from the fibre	Simple but low return power

The solution 1 needs a collimator of at least 70mm clear aperture, and the whole optical system will be very bulky. The cost to design and manufacture such a big size collimator with no chromatic aberration is very high, but it is very desirable for the FSI measurement.

For the solution 2, an automatic positioning mechanical system is required. This will reduce the measurement speed which definitely needs to be very fast. The external line measurement needs accurate knowledge of the position of launch optics, and then this solution is also excluded on principle.

Thus a fibre tip without any optic was chosen for the external short line measurement due to its simplicity, low cost and vanishing chromatic aberration. The disadvantage of this solution is that the power of the reflected light coupled

back into the fibre will be very small. In this paper, calculation and experimental results are reported, the high gain and low noise photo-detection unit is also described.

2. CALCULATIONS

2.1. Output optical field distribution from single mode fibre

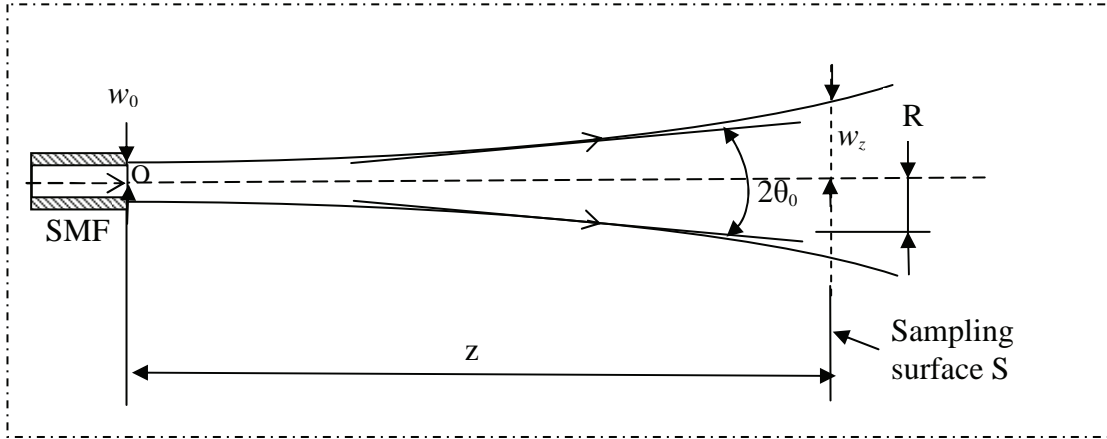


Figure 4: Output optical field distribution from single mode fibre

In order to know the level of the reflected light from the tunnel marker coupled back to the launching fibre, the calculation method based on Gaussian field distribution was used. It began with the optical field distribution of the light from a single mode fibre (SMF) (see Figure 4).

At a distance z from the fibre end, the radius of the $1/e^2$ intensity contour of the laser becomes

$$w_z = w_0 \left[1 + \left(\frac{\lambda z}{\pi w_0^2} \right)^2 \right]^{\frac{1}{2}}. \quad (5)$$

Here w_0 represents the radius of the laser waist.

When the distance z is much larger than the Rayleigh range,

$$w_z \approx \frac{\lambda z}{\pi w_0}. \quad (6)$$

The divergent angle of the laser beam, θ_0 , can be expressed by

$$\begin{aligned} \operatorname{tg} \theta_0 &= \frac{w_z}{z} \\ &\approx \frac{\lambda}{\pi w_0}. \end{aligned} \quad (7)$$

On the fibre end the light intensity at the central point is I_0 ; it becomes I_{0z} at the distance z . The output power P can be calculated by

$$\begin{aligned}
 P &= 2\pi I_0 \int_0^\infty e^{-2\left(\frac{r}{w_0}\right)^2} r dr = 2\pi I_{0z} \int_0^\infty e^{-2\left(\frac{r}{w_z}\right)^2} r dr \\
 &= 2\pi I_0 \int_0^\infty e^{-\left(\frac{\sqrt{2}}{w_0}\right)^2 r^2} r dr = 2\pi I_{0z} \int_0^\infty e^{-\left(\frac{\sqrt{2}}{w_z}\right)^2 r^2} r dr
 \end{aligned} \tag{8}$$

The integral

$$\int_0^\infty x e^{-a^2 x^2} dx = \frac{1}{2a^2} . \tag{9}$$

Thus

$$P = 2\pi I_0 \cdot \frac{1}{2\left(\frac{\sqrt{2}}{w_0}\right)^2} = 2\pi I_{0z} \cdot \frac{1}{2\left(\frac{\sqrt{2}}{w_z}\right)^2} . \tag{10}$$

So that

$$I_{0z} = \frac{w_0^2}{w_z^2} I_0 . \tag{11}$$

Then the light intensity at any point on the sampling surface S can be expressed by

$$\begin{aligned}
 I &= I_{0z} e^{-2\left(\frac{R}{w_z}\right)^2} \\
 &= \frac{w_0^2}{w_z^2} I_0 e^{-2\left(\frac{R}{w_z}\right)^2} ,
 \end{aligned} \tag{12}$$

where R is the off-axis distance of the point.

2.2. Fibre coupling efficiency

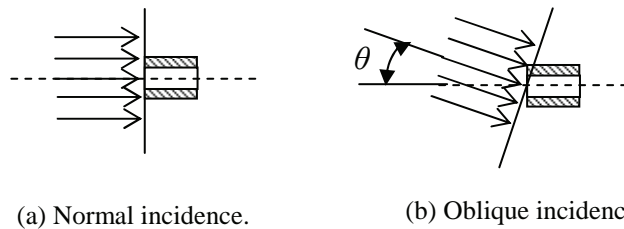


Figure 5: Coupling a plane wave light into a SMF

For a plane wave normal incident light (shown in Figure 5(a)), the effective collecting area of a single mode fibre, A_f , is

$$A_f = 2\pi r_0^2, \quad (13)$$

where r_0 is the mode-field radius of the fibre[8]. The collecting area is twice the area enclosed by the MFD (mode-field diameter).

If the incident light is oblique (shown in Figure 5(b)), the effective collecting area

$$A_f(\theta) = 2\pi r_0^2 e^{-2\left|\frac{\text{tg}\theta}{\text{tg}\theta_0}\right|^2}, \quad (14)$$

where θ is the light incident angle, and θ_0 is the divergent angle of the laser beam from the fibre (see equation 7).

If the incident light is emitted from the other SMF (shown in Figure 6), and z is much larger than Rayleigh range, the light at any point on S can be treated as plane wave.

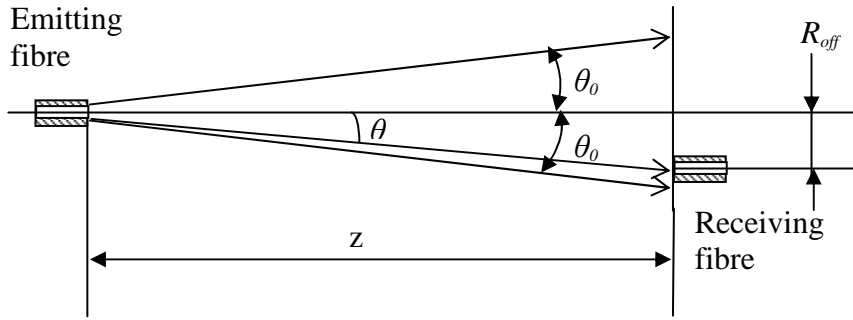


Figure 6: Coupling light from a SMF to a SMF

If the collecting fibre is at off-axis distance R_{off} , the power collected by it can be calculated as

$$\begin{aligned} P_c &= I_{off} \cdot 2\pi r_0^2 e^{-2\left|\frac{\text{tg}\theta}{\text{tg}\theta_0}\right|^2} \\ &= \frac{2w_0^2}{w_z^2} I_0 e^{-2\left(\frac{R_{off}}{w_z}\right)^2} \cdot \pi r_0^2 e^{-2\left|\frac{\text{tg}\theta}{\text{tg}\theta_0}\right|^2}. \end{aligned} \quad (15)$$

When the light is transmitted and collected by the fibres with identical mode fields, $w_0 = r_0$, then

$$P_c = \frac{2\pi w_0^4}{w_z^2} I_0 e^{-2\left(\frac{R_{off}}{w_z}\right)^2} e^{-2\left|\frac{\text{tg}\theta}{\text{tg}\theta_0}\right|^2}. \quad (16)$$

Thus the coupling efficiency

$$\begin{aligned}
C &= \frac{P_c}{P} \\
&= \frac{4w_0^2}{w_z^2} e^{-2\left(\frac{R_{off}}{w_z}\right)^2} e^{-2\left|\frac{tg\theta}{tg\theta_0}\right|^2},
\end{aligned} \tag{17}$$

where

$$tg\theta = \frac{R_{off}}{z}. \tag{18}$$

Substituting equation (6), (7) and (18) into equation (17), the coupling efficiency can be expressed by

$$C = \frac{4\pi^2 w_0^4}{\lambda^2 z^2} e^{-4\left(\frac{R_{off} \cdot \pi \cdot w_0}{\lambda \cdot z}\right)^2}. \tag{19}$$

2.3. Coupling efficiency versus the position of retro-reflector

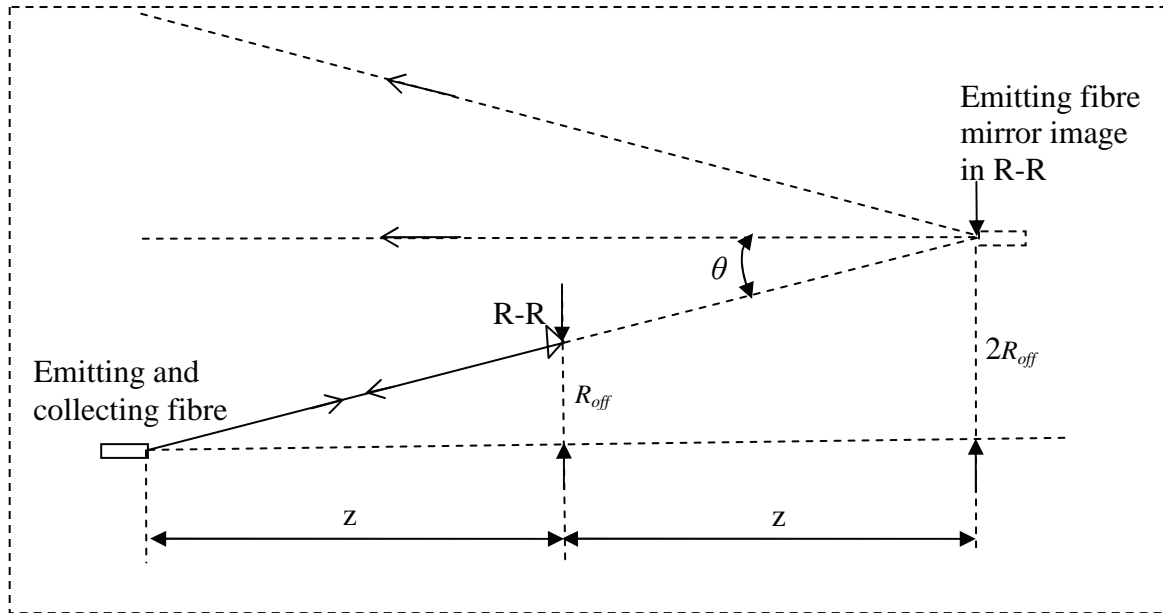


Figure 7: Coupling light reflected from a retro-reflector

In our set-up, the emitting fibre also receives the light after it has been reflected by the retro-reflector. The receiving fibre can be regarded as being located at the mirror location of the emitting fibre, see figure 7. The distance between the light source and the collecting fibre becomes $2z$, and the off-axis distance of the collecting fibre becomes $2R_{off}$. Then the coupling efficiency versus the position of retro-reflector is

$$C = \frac{4\pi^2 w_0^4}{\lambda^2 \cdot (2z)^2} \cdot e^{-4 \left(\frac{2R_{off} \cdot \pi \cdot w_0}{\lambda \cdot 2z} \right)^2}$$

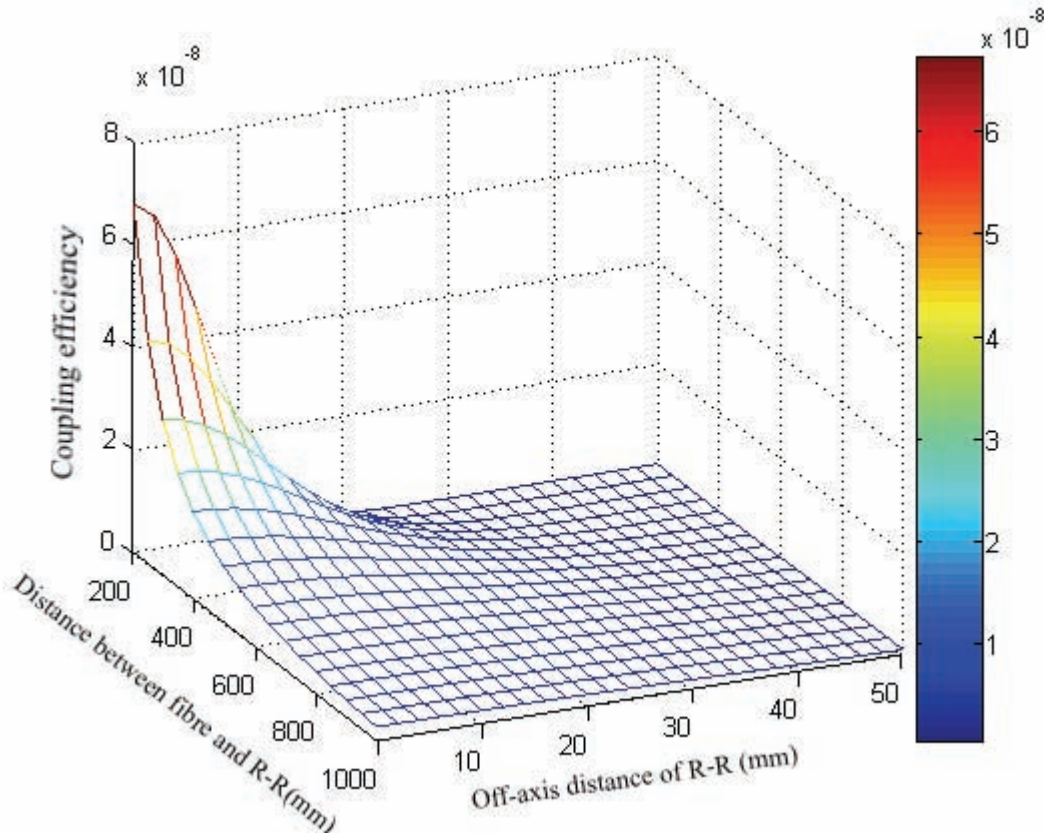
$$= \frac{\pi^2 w_0^4}{\lambda^2 z^2} \cdot e^{-4 \left(\frac{R_{off} \cdot \pi \cdot w_0}{\lambda \cdot z} \right)^2}, \quad (20)$$

Where z is the distance between the fibre tip and the retro-reflector, and R_{off} is the off-axis distance of the retro-reflector.

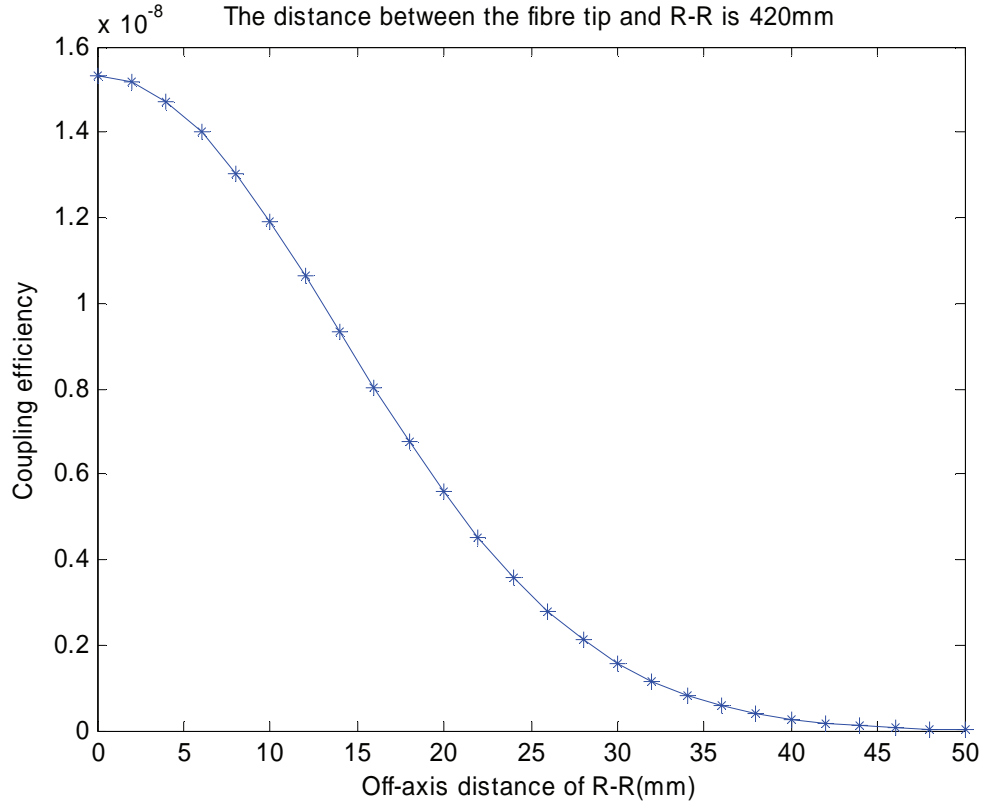
At 1550nm, the mode-field radius of SMF-28 fibre, w_0 , is 5.2 μ m. When z is 420mm, the radius of the light spot is 40mm (radius of the $1/e^2$ intensity contour, calculated by equation (6)). This meets the requirement of the external FSI system provided that the return light can be reliably detected in the entire field..

Results of the fibre coupling efficiency versus the position of retro-reflector (calculated by equation (20)) are shown in figure 8 (a) and (b).

When the retro-reflector is at $z = 420$ mm, the coupling efficiency of the reflected light from the retro-reflector back to the launching fibre will fall from 10^{-8} to 10^{-9} as the off-axis distance of the retro-reflector grows from 0 to 35mm. Then the return light is 16pW \sim 1pW when the output power of the fibre is 1mW.



(a)



(b)

Figure 8: Fibre coupling efficiency versus the position of R-R

3. PHOTO-DETECTION UNIT

When the frequency of the laser scans, the phase of a MI with OPD D is

$$\Theta(t) = \frac{2\pi}{c} D v(t) , \quad (21)$$

where $v(t)$ represents the laser frequency as a function of time and can be expressed as

$$v(t) = v_0 + \dot{v} \cdot t . \quad (22)$$

Here v_0 is the laser frequency at the start point. \dot{v} is the laser frequency scanning speed. In our application, the maximum laser frequency scanning speed is used. It is 5THz/s for the Agilent 81640A laser.

Then the frequency of the interference signal is

$$f_i = \frac{D}{C} \dot{v} . \quad (23)$$

The distance between the car and the retro-reflector is 400mm ~ 500mm, thus D for the short line FSI is 800mm~1000mm. Then the frequency of the interference signal is about 13.4kHz ~16.7kHz.

In order to detect the very weak interference signal, a photodiode/amplifier unit was designed to give sensitive detection of small fluctuations in intensity in the 1kHz to 25kHz frequency range, as shown in figure 9. The detector was an InGaAs PIN photodiode, Perkin-Elmer type C30617, with an ST optical fibre connector. The photodiode was

operated with a bias of approximately 4V, into a 100Mohm load resistor. This allowed for an optical input power up to 25nW before the bias voltage was unacceptably reduced.

The signal was buffered with a source follower using a 2N4416 JFET operating at 1.5mA, with a gain of 0.8 and a 300 ohm output impedance.

The signal from the source follower was amplified by two ac-coupled op-amp stages (Maxim MAX4180), to bring the input stage signal up to a convenient level for subsequent acquisition, and to correct and restrict the overall frequency response.

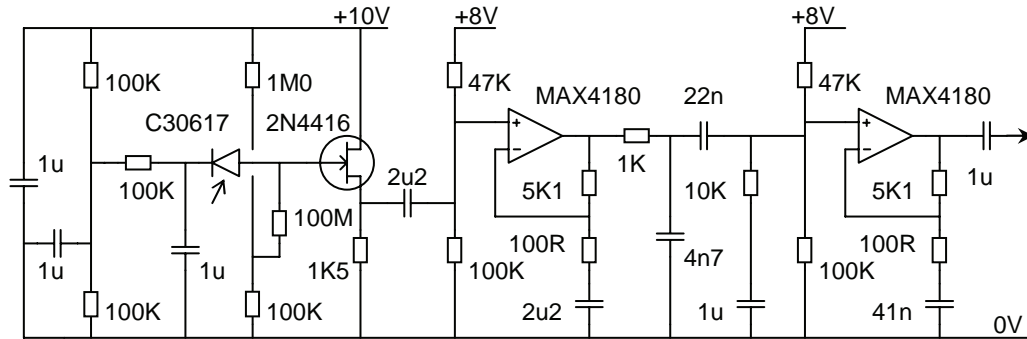


Figure 9: Circuit diagram of the photo-detection unit

4. EXPERIMENTAL RESULTS

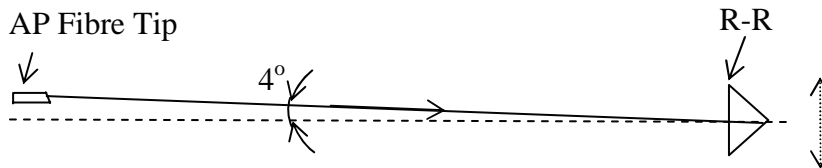


Figure 10: Set-up for the large area acceptance studies

In the short line FSI, the light reflected from the R-R interferes with the light reflected from the fibre tip. For a flat polished end fibre, around 4% of the light is reflected back at the end. When the output light power is 1mW, the reflected light from the flat end tip is about 40 μ W, much over the 25nW maximum optical input power of the photo-detection unit. A fibre with angle polished (AP) end is used here to form the short arm of the MI due to its low back reflection (high return loss > 60dB). The beam from the AP fibre deviates from the mechanical axis about 4 $^\circ$, as shown in Figure 10.

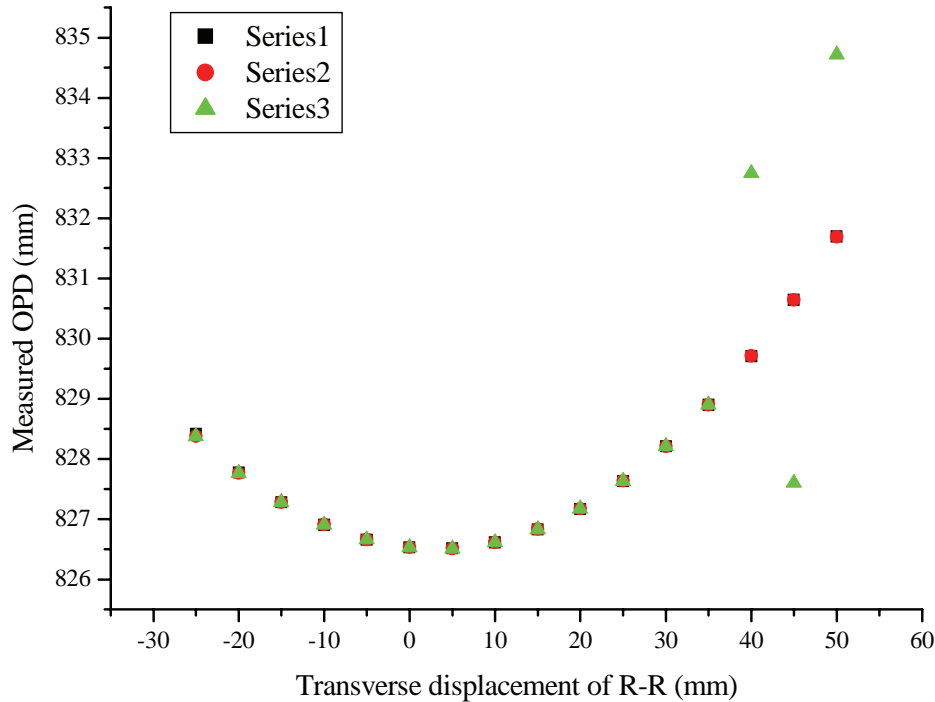


Figure 11: Measurement results

In the current set-up, a Michelson geometry interferometer is used as the reference interferometer, with a path length difference of approximate 4.7m. Light from an output channel of the fibre splitter tree is delivered to the interferometer via a 20m long fibre. An InGaAs photodiode detects the reference signal.

The retro-reflector was placed on a computer controlled linear stage for transverse motion in the large area acceptance study. In the experiment, the stage moved in steps of 5mm over a range of 90mm. At each stop, data of RI and MI signals were acquired, and then the OPD of the MI was calculated. Figure 11 shows 3 series of the OPD measurement results, indicating that the single mode fibre tip without any optic can cover a large measurement area of about 75mm diameter. Ignoring the three rightmost points of the green series, the standard deviation of the reconstructed OPD varies between $0.6\mu\text{m}$ and $6\mu\text{m}$.

5. CONCLUSIONS

Based on the FSI technique, a fibre sensor suitable for measuring the co-ordinates of the tunnel markers inside the ILC tunnel has been developed. In the measurement interferometer a fibre tip without any optic is used to launch and receive light to perform absolute distance measurements. Calculations indicate that the fibre coupling efficiency of the reflected light from the tunnel marker back to the launching fibre varies from 10^{-8} to 10^{-9} . A high gain and low noise photo-detection unit was designed to detect the very weak signals. Experimental results show that at ~420mm distance this fibre interferometer can cover a large measurement area of 75mm diameter.

References

- [1] G. Grzelak et al., “Simulation of the performance of the LiCAS train”, Proceedings of the 8th International Workshop on Accelerator Alignment, CERN, Switzerland/France, October 2004.
- [2] A. Reichold et al., “The LiCAS-RTRS – A Survey System for the ILC”, Proceedings of EPAC06, Edinburgh, June 2006, <http://www.epac06.org/>.
- [3] A. Mitra et al., “Measurement of the LiCAS systems”, Proceedings of the 8th International Workshop on Accelerator Alignment, CERN, Switzerland/France, October 2004.
- [4] A. Reichold et al., “The LiCAS-RTRS -A Rapid and Cost Efficient Survey System for the ILC”, Proceedings of the 9th International Workshop on Accelerator Alignment, SLAC, USA, September 2006.
- [5] G. Grzelak et al., “Simulation of the LiCAS Survey System for the ILC”, Proceedings of the 9th International Workshop on Accelerator Alignment, SLAC, USA, September 2006.
- [6] P. Coe et al., “Frequency scanning interferometry in ATLAS: remote, multiple, simultaneous and precise distance measurements in a hostile environment”, *Meas. Sci. Technol.* 15 (2004) 2175-2187.
- [7] J. Green, “An Automated Laser Metrology & Alignment System for the International Linear Collider”, to be published soon.
- [8] R. Bingham, “Analysis of defocus experiment”, October 2004.